Bulletin of Electrical Engineering and Informatics
Vol. 12, No. 3, June 2023, pp. 1773~1782
ISSN: 2302-9285, DOI: 10.11591/eei.v12i3.4848

COVID-19 classification using CNN-BiLSTM based on chest X-ray images

Denis Eka Cahyani[1], Anjar Dwi Hariadi[1], Faisal Farris Setyawan[1], Langlang Gumilar[2], Samsul Setumin[3]
[1]Department of Mathematics, Faculty of Mathematics and Natural Science, Universitas Negeri Malang, Malang, Indonesia
[2]Department of Electrical Engineering, Faculty of Engineering, Universitas Negeri Malang, Malang, Indonesia
[3]Centre for Electrical Engineering Studies, Universiti Teknologi MARA, Cawangan Pulau Pinang, Malaysia

Article Info

Article history:

Received Sep 23, 2022
Revised Dec 5, 2022
Accepted Dec 29, 2022

Keywords:

BiLSTM
Chest X-ray
CNN
COVID-19
Resnet50

ABSTRACT

Cases of the COVID-19 virus continue to spread still needs to be considered even though we have entered the post-pandemic era. Rapid identification of COVID-19 cases is necessary to prevent the virus from spreading further. This study developed a chest X-ray-based (CXR) COVID-19 classification for COVID-19 detection using the convolutional neural network-bidirectional long short-term memory (CNN-BiLSTM) combination model and compared the CNN-BiLSTM combination model with CNN models. The CNN models used in this study are the transfer learning models, namely Resnet50, VGG19, InceptionV3, Xception, and AlexNet. This research classifies CXR into three groups: COVID-19, normal, and viral pneumonia. In comparison to other models, the Resnet50-BiLSTM model is the most accurate and hence the best. The accuracy of the Resnet50-BiLSTM model was 98.48%. The model that obtains the next highest accuracy i.e Resnet50, VGG19-BiLSTM, VGG19, InceptionV3-BiLSTM, InceptionV3, Xception-BiLSTM, Xception, AlexNet-BiLSTM, and AlexNet. In this study, precision, recall, and F1-measure are also employed to demonstrate that Resnet50-BiLSTM achieves the highest value compared to other approaches. When compared to previous studies, this study enhances classification performance results.

Corresponding Author:

Denis Eka Cahyani
Department of Mathematics, Faculty of Mathematics and Natural Science, Universitas Negeri Malang
Jl. Semarang No. 5, Sumbersari, Lowokwaru, Malang, Jawa Timur 65145, Indonesia
Email: denis.eka.cahyani.fmipa@um.ac.id

1. INTRODUCTION

Cases of the COVID-19 virus continue to spread still needs to be considered even though we have entered the post-pandemic era. Several new varieties including omicron and delta are increasingly expanding in several nations [1], [2]. Therefore, it is vital to rapidly diagnose COVID-19 instances to prevent the virus's further transmission. Rapid screening with high sensitivity can aid health professionals in managing COVID-19 cases [3].

Multiple methods exist for detecting COVID-19 infections, including chest or lung X-rays. Radiological testing can detect alterations in the human lung prior to and after the onset of COVID-19 symptoms [4]. A person infected with the COVID-19 virus has irregular air space opacities in either the right or left lung which can be detected from radiological examination [5]. The types of radiological examinations include computed tomography (CT) scan, chest X-ray (CXR), and ultrasonography (USG) of the lungs [6]. CXR has the advantage of being more accessible because every hospital has CXR facilities, compared to other types of radiological examinations such as CT scan and ultrasound of the lungs. In addition, CXR has an effectiveness rate of up to 89 percent in detecting the COVID-19 virus [7].

This research employs the COVID-19 radiography database [8], [9] to identify the COVID-19 virus in CXR data. More than 10,000 CXR images in positive instances of COVID-19, viral pneumonia, and normal are included in the collection. With the introduction of deep learning, it is now easier to assess enormous volumes of available data. Convolutional neural networks (CNN) are a popular deep learning method in the medical field.

Previous research has generated CNN image categorization models such as GoogleNet [10], [11], VGGNet [12], [13], ResNet [14], [15], and AlexNet [16], [17]. As performed by Ardakani *et al.* [18], the CNN approach can be utilized to detect COVID-19 instances by differentiating between CXR images that are infected with COVID19 and those that are not infected with COVID-19. Furthermore, Rahaman *et al.* [19] used CXR images for COVID-19 detection by comparing CNN models such as VGG19, Alexnet, Resnet 50, and DenseNet. There are limits to these investigations employing simply the CNN model for image recognition. However, the CNN model allows it to be combined with other deep learning models to get better model performance. Imaduddin *et al.* [20] also conducted research about the detection of COVID-19 in CXR data. Imaduddin *et al.* [20] is restricted to using only the normal class and COVID-19 class of data. The volume of research data must be raised so that the COVID-19 detection model yields higher performance results. This study utilizes the same dataset as the study [20], but it employs three classifications, namely COVID-19, normal, and viral pneumonia, resulting in a greater quantity of data than the study [20].

The CNN model can learn local responses from image data so that it can extract data features in parallel, but CNN has the disadvantage that it cannot learn sequential correlation of data [21]. On the other hand, recurrent neural networks (RNN) is advantageous for sequence data modeling, but cannot extract data characteristics in parallel [22]. One of the RNN models is bidirectional long short-term memory (BiLSTM). BiLSTM is advantageous for sequence data modeling, however it cannot extract data characteristics in parallel [23]. Deep learning methods such as CNN and BiLSTM can be combined by taking advantage of the advantages of each method to obtain a more accurate deep learning model.

Research has developed a combination of CNN and BiLSTM for other cases such as sentiment document analysis [24], stock price prediction [25], [26], and document text classification [27], [28]. Research related to the combination of CNN and BiLSTM for COVID-19 detection has been carried out by Aslan *et al.* [29] but this study only uses the AlexNet-BiLSTM for the identification of COVID-19 infection. This research uses several transfer learning models on CNN, not only AlexNet-BiLSTM, but also Resnet50-BiLSTM, VGG19-BiLSTM, InceptionV3-BiLSTM and Xception-BiLSTM. Therefore, the contribution in this research is to combine the CNN models (Resnet50, VGG19, InceptionV3, Xception, and AlexNet) with BiLSTM for automated COVID-19 detection based on CXR images and compare the CNN-BiLSTM combination model with a CNN model that does no combined with BiLSTM. By comparing the CNN-BiLSTM with the CNN model, it will produce a performance comparison between models so that you can choose the best model to detect COVID-19.

This study aims to establish a COVID-19 categorization based on CXR data using a combination of CNN models (Resnet50, VGG19, InceptionV3, Xception, AlexNet) and BiLSTM for early detection of patients infected with the COVID-19 virus effectively. The combination of CNN and BiLSTM models is expected to detect COVID-19 more accurately. Health workers can be assisted in detecting the COVID-19 virus in patients. Patients can be treated quickly to receive appropriate treatment so that the spread of the COVID-19 virus can be prevented more widely.

2. MATERIAL AND METHOD

Based on X-ray images, this study presented a categorization of COVID-19. The classification model was developed in this study using a combination of CNN and BiLSTM. The research method consists of pre-processing data, modeling data, hyperparameter tuning, and model evaluation. The evaluation model uses a confusion matrix by calculating accuracy, precision, recall, and F1-measure.

2.1. Dataset

COVID-19 radiography database is the data source for this investigation. The collection contains three categories of CXR images, namely COVID-19, normal, and viral pneumonia. Figure 1 depicts an example CXR image from the dataset. Figure 1(a) shows an example of COVID-19 CXR image, Figure 1(b) shows an example of normal CXR image, and Figure 1(c) shows an example of pneumonia CXR image. Table 1 depicts the distribution of training and testing data for the dataset. 8:2 data ratio is applied to training and examination data.

(a) (b) (c)

Figure 1. An example of COVID-19, normal, and pneumonia in CXR images (a) COVID-19 CXR, (b) normal CXR, and (c) pneumonia CXR

Table 1. The dataset applied in this study

Dataset/class	COVID-19	Normal	Viral pneumonia	Total
Train	2,893	8,154	1,076	12,123
Test	723	2,038	269	3,030
Total	3,616	10,192	1,345	15,153

2.2. Data pre-processing

The image is resized to 224×224 pixels so that the images have the same size. Augmentation technique is also applied at the pre-processing stage by using Keras “ImageDataGenerator”. This augmentation technique is applied to improve the performance of the proposed model. Additionally, horizontal flip is utilized to horizontally flip the image's rows and columns. Moreover, rescale is employed at rescale 1/255 to alter the scale of image values. Then, validation split=0.2 is used to divide data into training and validation sets.

2.3. Data modeling

This study developed a combination classification model for CNN and BiLSTM. Resnet50, VGG19, InceptionV3, Xception, and AlexNet are the transfer learning CNN models utilized in this research. Each CNN model is combined with the BiLSTM model. Then the CNN-BiLSTM combination model is compared with the CNN-BiLSTM model alone which is not combined with BiLSTM. Jupyter Notebook, python 3.10, a Core i7 processor, 16 GB of RAM with a speed of 3,600 MHz, and an Nvidia Cuda GPU are utilized in this study for building the model.

The CNN-BiLSTM models used in this study are Resnet50-BiLSTM, VGG19-BiLSTM, InceptionV3-BiLSTM, Xception-BiLSTM, and AlexNet-BiLSTM. CNN-BiLSTM models are comprised of previously trained models that have been trained on the ImageNet dataset. Imported Keras models contain convolutional layers for extracting visual characteristics. The size of network inputs is (224, 224, and 3). The CNN-BiLSTM model only uses convolutional layers in the pre-trained model so that other layers in the previously learned model are removed such as the flatten layer, fully connected layer (FCL), and softmax activation layer. The layer is modified by adding a flatten layer to convert the two-dimensional feature matrix into a vector. Then added BiLSTM with 128 units. A dropout layer was also added to control overfitting with a dropout of 0.5. The BiLSTM layer and the dropout layer are repeated twice. Furthermore, the amount of neurons, 128, is added to the FCL which has an activation function. Next, the dropout layer is added again. Finally, the final layer of the CNN architecture generates an output image categorization using the softmax function. The architecture of the Resnet50-BiLSTM model is shown in Figure 2.

This study compares the CNN-BiLSTM with the CNN model. The CNN models used in this study are Resnet50, VGG19, InceptionV3, Xception, and AlexNet. The CNN model used in this work was previously trained on the ImageNet dataset. Imported Keras models contain convolutional layers for extracting visual characteristics. The size of network inputs is (224, 224, and 3). After the convolutional layer, the flatten layer is applied to turn the feature matrix into a vector. In addition, the FCL is added using the activation function tanh and 128 neurons. To generate output for image categorization, a softmax activation layer is applied at the end.

2.4. Hyperparameter tuning

In the hyperparameter tuning phase, the optimal experimental scenario parameters are determined. Loss function, optimizer, batch size, model activation, and epoch are the parameters utilized in this investigation. Categorical crossentropy is the loss function applied in this study. Stochastic gradient descent (SGD) is employed as the optimizer. The batch size utilized is 16. 10 is used as the epoch. Then, the tanh activation model is employed.

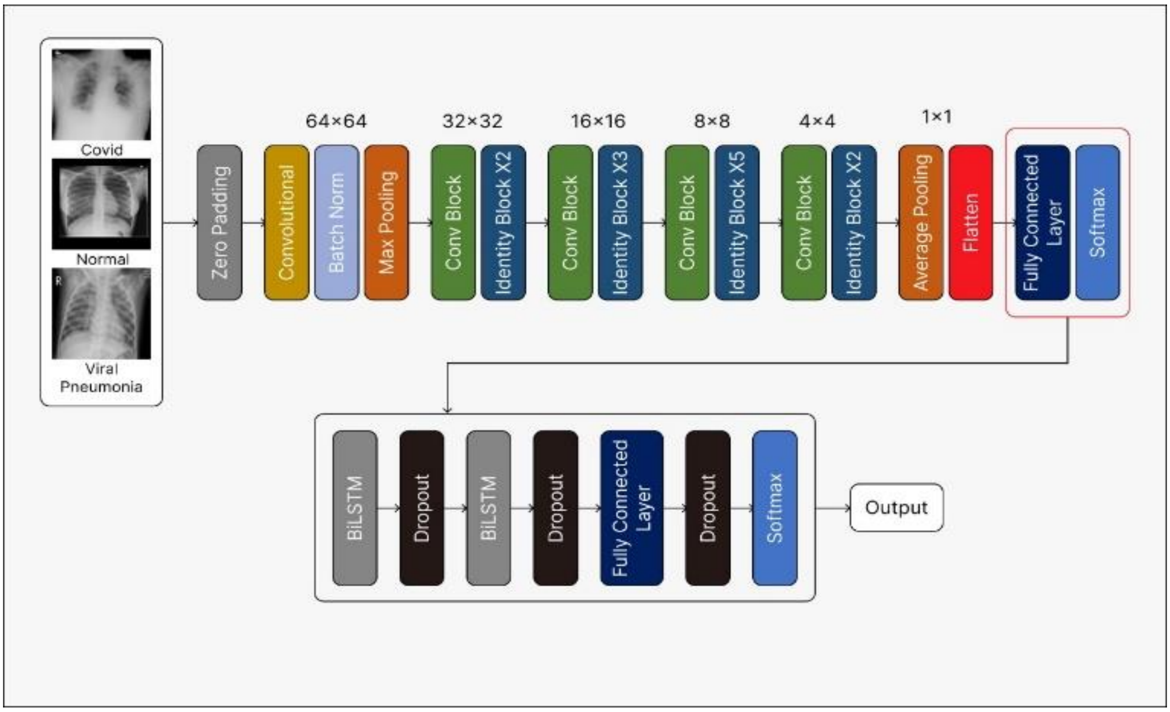

Figure 2. The Resnet50-BiLSTM architecture

3. RESULTS AND DISCUSSION

This study employs ten experimental categorization scenarios for COVID-19 based on CXR data. The experimental scenarios used are Resnet50-BiLSTM, VGG19-BiLSTM, InceptionV3-BiLSTM, Xception-BiLSTM, AlexNet-BiLSTM, Resnet50, VGG19, InceptionV3, Xception, and AlexNet. Figure 3 depicts a comparison of the study's accuracy. In comparison to other models, the Resnet50-BiLSTM model delivers the most accurate results. The accuracy of the Resnet50-BiLSTM model was 98.48%. The model that obtains the next highest accuracy i.e Resnet50, VGG19-BiLSTM, VGG19, InceptionV3-BiLSTM, InceptionV3, Xception-BiLSTM, Xception, and AlexNet-BiLSTM. The AlexNet model obtained the lowest accuracy of 94.79% compared to other models.

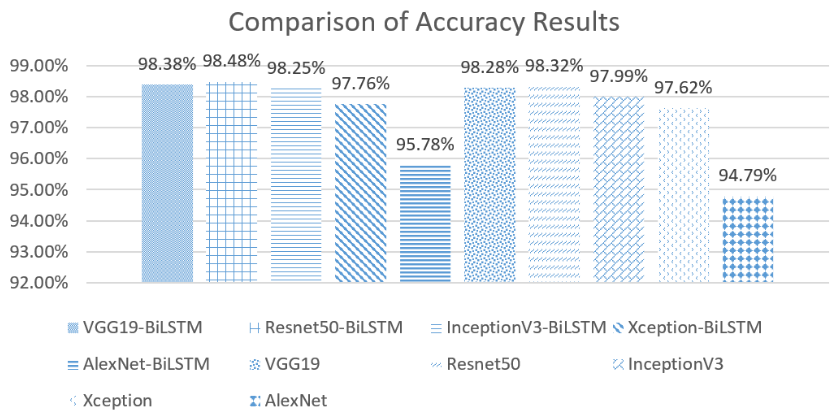

Figure 3. The comparison of accuracy results

Precision, recall, and F1-measure are also employed in the evaluation of this study. The purpose of the evaluation is to assess the performance of the detection model using COVID-19 CXR data. The comparison of precision, recall, and F1-measure is presented in Table 2. Comparing precision, recall, and F1-measure reveals that Resnet50-BiLSTM achieves the greatest value compared to other approaches. Precision, recall, and F1-measure are 98.54%, 98.48%, and 98.50%, respectively, for Resnet50-BiLSTM. Then followed further models, specifically VGG19-BiLSTM, Resnet50, VGG19, InceptionV3-BiLSTM, InceptionV3, Xception-BiLSTM, Xception, AlexNet-BiLSTM, and AlexNet.

Table 2. The comparison of precision, recall, and F1-measure

Model	Precision (%)	Recall (%)	F1-measure (%)
VGG19-BiLSTM	98.40	98.38	98.38
Resnet50-BiLSTM	98.54	98.48	98.50
InceptionV3-BiLSTM	98.27	98.25	98.24
Xception-BiLSTM	97.83	97.76	97.77
AlexNet-BiLSTM	95.79	95.78	95.78
VGG19	98.30	98.28	98.29
Resnet50	98.37	98.32	98.33
InceptionV3	98.00	97.99	97.96
Xception	97.68	97.62	97.64
AlexNet	95.03	94.79	94.84

In this study, the confusion matrix test data is presented so that the performance of each model may be evaluated in detail. The Resnet50-BiLSTM model, which has the best accuracy, is able to distinguish 710 photos in the COVID-19 class, despite detecting 10 images in the normal class and 3 images in the viral pneumonia class. In the usual picture class, the detection of 2009 photos was accurate. However, 6 pictures were identified as belonging to the COVID-19 class and 23 as belonging to the pneumonia class. In the pneumonia class, 265 photos were successfully identified. Nonetheless, four photos were wrongly classified as normal. The AlexNet model with the lowest accuracy score is able to classify 697 COVID-19 pictures, while 24 are classified as normal and 2 as viral pneumonia. 1931 images may be properly identified as belonging to the normal image class, 96 as belonging to the COVID-19 class, and 11 as belonging to the pumonia class. 244 photographs in the pumonia class were accurately identified, whereas 5 images were identified as COVID-19 class and 20 as normal class. The justification for applying Resnet50-BiLSTM for the chesy X-Ray-based COVID-19 classification is therefore strengthened. Figure 4 displays alternative confusion matrix models. Figure 4(a) depicts VGG19-BiLSTM confusion matrix, Figure 4(b) Resnet50-BiLSTM confusion matrix, Figure 4(c) InceptionV3-BiLSTM confusion matrix, and Figure 4(d) Xception-BiLSTM confusion matrix, Figure 4(e) AlexNet-BiLSTM confusion matrix, Figure 4(f) VGG19 confusion matrix, Figure 4(g) Resnet50 confusion matrix, Figure 4(h) InceptionV3 confusion matrix, Figure 4(i) Xception confusion matrix, and Figure 4(j) AlexNet confusion matrix.

In this study, accuracy curves are provided to illustrate the performance of the model at each epoch. Figure 5 (in Appendix) illustrates the accuracy curves for every model. Figure 5(a) illustrates the accuracy curves for VGG19-BiLSTM, Figure 5(b) for Resnet50-BiLSTM, Figure 5(c) for InceptionV3-BiLSTM, Figure 5(d) for Xception-BiLSTM, Figure 5(e) for AlexNet-BiLSTM, Figure 5(f) for VGG19, Figure 5(g) for Resnet50, Figure 5(h) for InceptionV3, and Figure 5(i) for Xception. The Resnet50-BiLSTM curve has a stable curve and has high training and validation accuracy. From 0 to 10 epochs, the accuracy curve of the training data rises around 99.9% every epoch. In the meanwhile, the val accuracy curve exhibits a sudden increase from epoch 0 to epoch 1 at a rate of 90%, followed by a fall in val accuracy in the subsequent epoch, followed by a steady growth at a rate of around 98%. In the 8th epoch, the val accuracy value decreased to 82% and then rose slowly and steadily at around 98%. In contrast to the accuracy curve of the Resnet50-BiLSTM model, the AlexNet-BiLSTM model shows an overfitting accuracy curve. From epochs 1 to 10, the accuracy curve in the training data improves in value, but the val accuracy curve exhibits erratic increases. In the val accuracy value, there is a decrease in epochs 2 and 4, then the curve moves up with a value of around 94%.

According to the results, the Resnet50-BiLSTM model had the best performance compared to the other models. This is because the Resnet50-BiLSTM architecture combines the Resnet50 model and the BiLSTM model. The Resnet50 model has the advantage of being able to study local responses from image data so that it can extract features of CXR images in parallel well. While the BiLSTM model has advantages in sequential data modeling so that it is accurate in classifying data. Therefore, the combination of Resnet50 and BiLSTM models has the advantages of the two models so that it has better model performance than other models. The combination of CNN and BiLSTM models in this study resulted in better performance than the CNN model alone which was not combined with BiLSTM. This indicates that the BiLSTM model combined with the CNN model has an effect on improving the performance of the CXR images-based COVID-19 classification model.

Test data confusion matrix

True Label	COVID-19	Normal	Pneumonia
COVID-19	698	23	2
Normal	7	2018	13
Pneumonia	1	3	265
	Predicted Label		

(a)

Test data confusion matrix

True Label	COVID-19	Normal	Pneumonia
COVID-19	710	10	3
Normal	6	2009	23
Pneumonia	0	4	265
	Predicted Label		

(b)

Test data confusion matrix

True Label	COVID-19	Normal	Pneumonia
COVID-19	693	29	1
Normal	1	2033	4
Pneumonia	0	18	251
	Predicted Label		

(c)

Test data confusion matrix

True Label	COVID-19	Normal	Pneumonia
COVID-19	689	28	6
Normal	3	2012	23
Pneumonia	0	8	261
	Predicted Label		

(d)

Test data confusion matrix

True Label	COVID-19	Normal	Pneumonia
COVID-19	682	40	1
Normal	49	1974	15
Pneumonia	5	18	246
	Predicted Label		

(e)

Test data confusion matrix

True Label	COVID-19	Normal	Pneumonia
COVID-19	700	21	2
Normal	8	2015	15
Pneumonia	2	4	263
	Predicted Label		

(f)

Test data confusion matrix

True Label	COVID-19	Normal	Pneumonia
COVID-19	706	16	1
Normal	8	2007	23
Pneumonia	0	3	266
	Predicted Label		

(g)

Test data confusion matrix

True Label	COVID-19	Normal	Pneumonia
COVID-19	704	17	2
Normal	6	2029	3
Pneumonia	0	33	236
	Predicted Label		

(h)

Test data confusion matrix

True Label	COVID-19	Normal	Pneumonia
COVID-19	701	19	3
Normal	17	1995	26
Pneumonia	0	7	262
	Predicted Label		

(i)

Test data confusion matrix

True Label	COVID-19	Normal	Pneumonia
COVID-19	697	24	2
Normal	96	1931	11
Pneumonia	5	20	244
	Predicted Label		

(j)

Figure 4. The model results of the confusion matrix (a) VGG19-BiLSTM, (b) Resnet50-BiLSTM, (c) InceptionV3-BiLSTM, (d) Xception-BiLSTM, (e) AlexNet-BiLSTM, (f) VGG19, (g) Resnet50, (h) InceptionV3, (i) Xception, and (j) AlexNet

The CNN models compared in this study are Resnet50, VGG19, InceptionV3, Xception, and AlexNet. The Resnet50 model generated the best results in comparison to other models. Due to the Resnet50 architecture, which leverages a shortcut connection idea to prevent considerable information loss during training, this is the case. To enhance model performance, it is not practical to simply stack layers while constructing the model architecture. The higher the depth of a network, the greater the chance of vanishing gradient, which causes the gradient to become extremely tiny, resulting in reduced performance or accuracy [10]. ResNet therefore developed the notion of shortcut connections as a means of minimizing the loss of key characteristics during the convolution procedure.

This study's examination of model performance improves performance outcomes in comparison to previous research [20]. The accuracy, precision, and F1-measure of the Resnet50 model generated by prior research are 93.3%, 93%, and 93%, respectively. The Resnet50 model is the best model produced by earlier research [20]. CNN and BiLSTM have not been coupled in prior research. The findings of this investigation reveal that the model with the greatest performance is Resnet50-BiLSTM. The Resnet50-BiLSTM model produces precision, accuracy, and F1-measures of 98.48%, 98.54%, and 98.50%, respectively. As a consequence, the performance of COVID-19 detection utilizing CXR images is enhanced in this study.

4. CONCLUSION

This study successfully classified COVID-19 using CXR data using a combination of CNN and BiLSTM. The CNN models used in this study are Resnet50, VGG19, InceptionV3, Xception, and AlexNet. This study uses ten experimental scenarios for COVID-19 categorization based on CXR data, namely Resnet50-BiLSTM, VGG19-BiLSTM, InceptionV3-BiLSTM, Xception-BiLSTM, AlexNet-BiLSTM, Resnet50, VGG19, InceptionV3, Xception, and AlexNet. This research classifies CXRs into three groups: COVID-19, normal, and viral pneumonia. In comparison to other models, the Resnet50-BiLSTM model is the most accurate and hence the best. The accuracy of the Resnet50-BiLSTM model was 98.48%. The model that obtains the next highest accuracy i.e Resnet50, VGG19-BiLSTM, VGG19, InceptionV3-BiLSTM, InceptionV3, Xception-BiLSTM, Xception, AlexNet-BiLSTM, and AlexNet. In this study, precision, recall, and F1-measure are also employed to demonstrate that Resnet50-BiLSTM achieves the highest value compared to other approaches. Comparing the performance of alternative transfer learning models in CNN, such as DenseNet or GoogleNet, with the performance of the transfer learning models in this study would require more investigation. In addition, further research can develop a web-based application with the Django framework for classification of COVID-19 based on CXR data.

ACKNOWLEDGEMENTS

We would like to thank the Institute for Research and Community Service (LP2M) Universitas Negeri Malang for providing the 2022 research grant funds. This paper is used as a mandatory outcome of the 2022 research grant as well as a form of accountability for the research grant. Thanks also to fellow researchers who have helped this research to achieve the best results.

APPENDIX

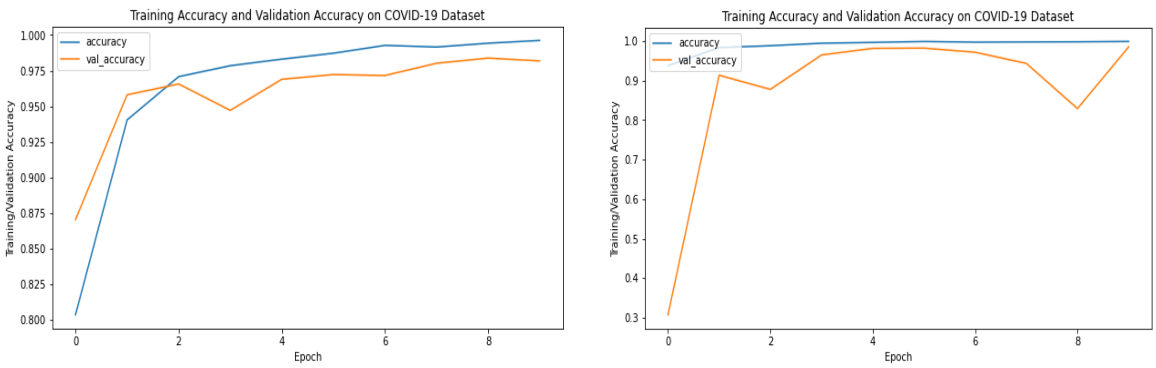

(a) (b)

Figure 5. The accuracy curve in models (a) VGG19-BiLSTM, (b) Resnet50-BiLSTM

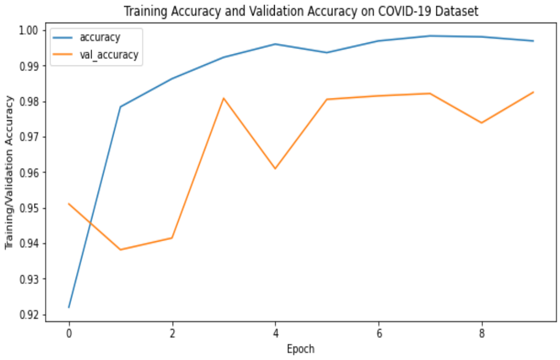

(c)

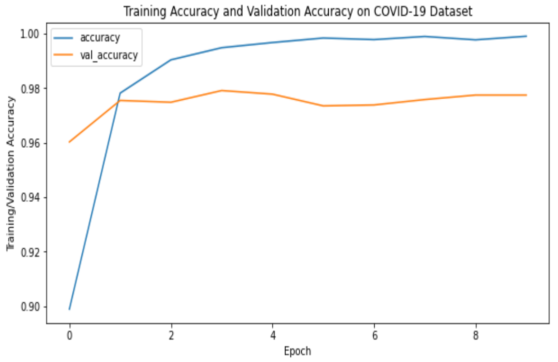

(d)

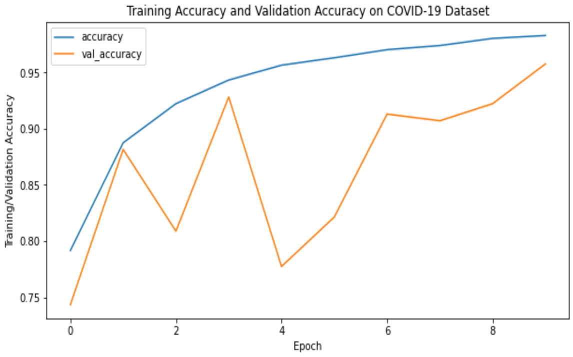

(e)

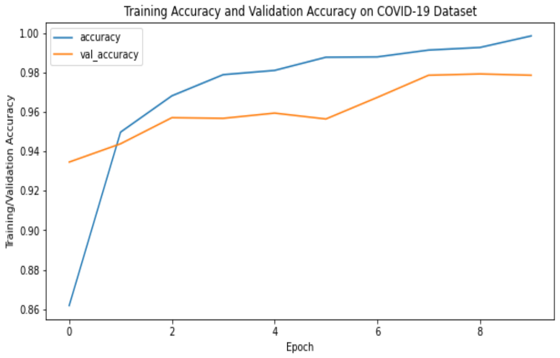

(f)

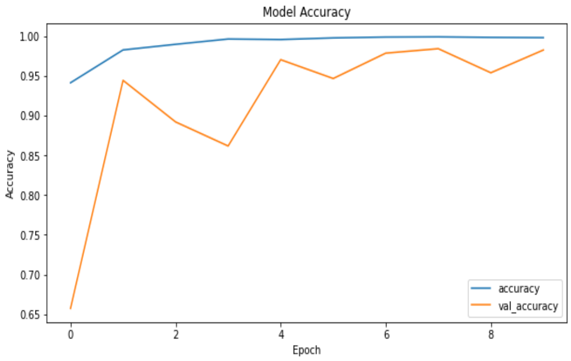

(g)

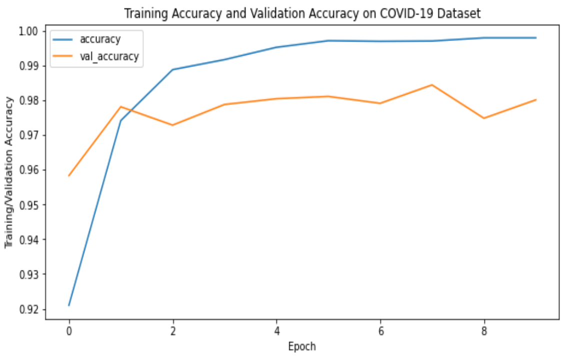

(h)

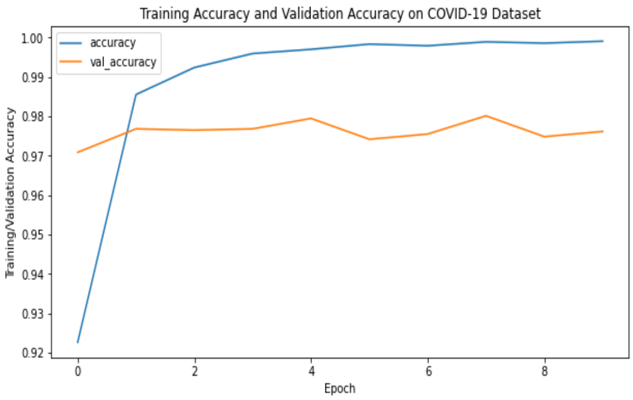

(i)

Figure 5. The accuracy curve in models (c) InceptionV3-BiLSTM, (d) Xception-BiLSTM, (e) AlexNet-BiLSTM, (f) VGG19, (g) Resnet50, (h) InceptionV3, and (i) Xception (continue)

REFERENCES

[1] S. S. A. Karim and Q. A. Karim, "Omicron SARS-CoV-2 variant: a new chapter in the COVID-19 pandemic," *The Lancet*, vol. 398, no. 10317, pp. 2126–2128, Dec. 2021, doi: 10.1016/s0140-6736(21)02758-6.

[2] M. Ravisankar, S. Alexandar, R. S. Kumar, and K. Jakkan, "A Comprehensive Review on Covid-19 Delta variant," *International Journal of Pharmacology and Clinical Research (IJPCR)*, vol. 5, no. 2, 2021.

[3] M. K. Pandit and S. A. Banday, "SARS n-CoV2-19 detection from chest x-ray images using deep neural networks," *International Journal of Pervasive Computing and Communications*, vol. 16, no. 5, pp. 419–427, Jul. 2020, doi: 10.1108/ijpcc-06-2020-0060.

[4] L. Hu and C. Wang, "Radiological role in the detection, diagnosis and monitoring for the coronavirus disease 2019 (COVID-19)," *Eur Rev Med Pharmacol Sci*, vol. 24, no. 8, pp. 4523–4528, Apr. 2020, doi: 10.26355/eurrev_202004_21035.

[5] W. Kong and P. P. Agarwal, "Chest Imaging Appearance of COVID-19 Infection," *Radiology: Cardiothoracic Imaging*, vol. 2, no. 1, p. e200028, Feb. 2020, doi: 10.1148/ryct.2020200028.

[6] T. Riawati, W. Indrarto, A. R. Fauzi, W. Widitjiarso, and Gunadi, "Various radiological findings in patients with COVID-19: A case series," *Annals of Medicine and Surgery*, vol. 62, pp. 269–273, Feb. 2021, doi: 10.1016/j.amsu.2021.01.030.

[7] V. N. M. Aradhya, M. Mahmud, B. Agarwal, D. S. Guru, and M. S. Kaiser, "One Shot Cluster Based Approach for the Detection of COVID-19 from Chest X-Ray Images," Jul. 2020, doi: 10.20944/preprints202007.0656.v1.

[8] M. E. H. Chowdhury *et al.*, "Can AI Help in Screening Viral and COVID-19 Pneumonia?," *IEEE Access*, vol. 8, pp. 132665–132676, 2020, doi: 10.1109/access.2020.3010287.

[9] M. Nishio, "Review of: 'Exploring the effect of image enhancement techniques on COVID-19 detection using chest X-ray images," Qeios Ltd, Nov. 2021, doi: 10.32388/xyk0mg.

[10] N. Alsharman and I. Jawarneh, "GoogleNet CNN Neural Network towards Chest CT-Coronavirus Medical Image Classification," *Journal of Computer Science*, vol. 16, no. 5, pp. 620–625, May 2020, doi: 10.3844/jcssp.2020.620.625.

[11] N. A. Muhammad, A. A. Nasir, Z. Ibrahim, and N. Sabri, "Evaluation of CNN, Alexnet and GoogleNet for Fruit Recognition," *Indonesian Journal of Electrical Engineering and Computer Science*, vol. 12, no. 2, p. 468, Nov. 2018, doi: 10.11591/ijeecs.v12.i2.pp468-475.

[12] C. Sitaula and M. B. Hossain, "Attention-based VGG-16 model for COVID-19 chest X-ray image classification," *Applied Intelligence*, vol. 51, no. 5, pp. 2850–2863, Nov. 2020, doi: 10.1007/s10489-020-02055-x.

[13] Y. Zhang *et al.*, "Deep learning model for classifying endometrial lesions," *Journal of Translational Medicine*, vol. 19, no. 1, Jan. 2021, doi: 10.1186/s12967-020-02660-x.

[14] S. Bharati, P. Podder, M. R. H. Mondal, and V. B. S. Prasath, "CO-ResNet: Optimized ResNet model for COVID-19 diagnosis from X-ray images," *International Journal of Hybrid Intelligent Systems*, vol. 17, no. 1–2, pp. 71–85, Jul. 2021, doi: 10.3233/his-210008.

[15] L. Wen, X. Li, and L. Gao, "A transfer convolutional neural network for fault diagnosis based on ResNet-50," *Neural Computing and Applications*, vol. 32, no. 10, pp. 6111–6124, Feb. 2019, doi: 10.1007/s00521-019-04097-w.

[16] S. Samir, E. Emary, K. El-Sayed, and H. Onsi, "Optimization of a Pre-Trained AlexNet Model for Detecting and Localizing Image Forgeries," *Information*, vol. 11, no. 5, p. 275, May 2020, doi: 10.3390/info11050275.

[17] E. Cortes and S. Sanchez, "Deep Learning Transfer with AlexNet for chest X-ray COVID-19 recognition," *IEEE Latin America Transactions*, vol. 19, no. 6, pp. 944–951, Jun. 2021, doi: 10.1109/tla.2021.9451239.

[18] A. A. Ardakani, A. R. Kanafi, U. R. Acharya, N. Khadem, and A. Mohammadi, "Application of deep learning technique to manage COVID-19 in routine clinical practice using CT images: Results of 10 convolutional neural networks," *Computers in Biology and Medicine*, vol. 121, p. 103795, Jun. 2020, doi: 10.1016/j.compbiomed.2020.103795.

[19] M. M. Rahaman *et al.*, "Identification of COVID-19 samples from chest X-Ray images using deep learning: A comparison of transfer learning approaches," *Journal of X-Ray Science and Technology*, vol. 28, no. 5, pp. 821–839, Sep. 2020, doi: 10.3233/xst-200715.

[20] H. Imaduddin, F. Y. Ala, A. Fatmawati, and B. A. Hermansyah, "Comparison of transfer learning method for COVID-19 detection using convolution neural network," *Bulletin of Electrical Engineering and Informatics*, vol. 11, no. 2, pp. 1091–1099, Apr. 2022, doi: 10.11591/eei.v11i2.3525.

[21] Y. Lu and J. Yan, "Automatic Lip Reading Using Convolution Neural Network and Bidirectional Long Short-Term Memory," *Intern J Pattern Recognit Artif Intell*, vol. 34, no. 1, Jan. 2020, doi: 10.1142/S0218001420540038.

[22] A. L. Caterini and D. E. Chang, "Recurrent Neural Networks," in *Deep Neural Networks in a Mathematical Framework*, Springer International Publishing, 2018, pp. 59–79, doi: 10.1007/978-3-319-75304-1_5.

[23] K. Zhao, L. Huang, R. Song, Q. Shen, and H. Xu, "A Sequential Graph Neural Network for Short Text Classification," *Algorithms*, vol. 14, no. 12, p. 352, Dec. 2021, doi: 10.3390/a14120352.

[24] M. Rhanoui, M. Mikram, S. Yousfi, and S. Barzali, "A CNN-BiLSTM Model for Document-Level Sentiment Analysis," *Machine Learning and Knowledge Extraction*, vol. 1, no. 3, pp. 832–847, Jul. 2019, doi: 10.3390/make1030048.

[25] Y. Chen *et al.*, "Stock Price Forecast Based on CNN-BiLSTM-ECA Model," *Scientific Programming*, vol. 2021, pp. 1–20, Jul. 2021, doi: 10.1155/2021/2446543.

[26] W. Lu, J. Li, J. Wang, and L. Qin, "A CNN-BiLSTM-AM method for stock price prediction," *Neural Computing and Applications*, vol. 33, no. 10, pp. 4741–4753, Nov. 2020, doi: 10.1007/s00521-020-05532-z.

[27] W. Meng, Y. Wei, P. Liu, Z. Zhu, and H. Yin, "Aspect Based Sentiment Analysis With Feature Enhanced Attention CNN-BiLSTM," *IEEE Access*, vol. 7, pp. 167240–167249, 2019, doi: 10.1109/access.2019.2952888.

[28] Y. Zeng, R. Zhang, L. Yang, and S. Song, "Cross-Domain Text Sentiment Classification Method Based on the CNN-BiLSTM-TE Model," *Journal of Information Processing Systems*, vol. 17, no. 4, pp. 818–833, 2021, doi: 10.3745/JIPS.04.0221.

[29] M. F. Aslan, M. F. Unlersen, K. Sabanci, and A. Durdu, "CNN-based transfer learning–BiLSTM network: A novel approach for COVID-19 infection detection," *Applied Soft Computing*, vol. 98, p. 106912, Jan. 2021, doi: 10.1016/j.asoc.2020.106912.

BIOGRAPHIES OF AUTHORS

Denis Eka Cahyani holds a Bachelor of Computer Science (S. Kom.) in Computer Science, Master of Computer Science (M.Kom.) in Computer Science, Universitas Indonesia in 2015 besides several professional certificates and skills. She holds a Bachelor of Informatics degree from Universitas Sebelas Maret, Indonesia in 2013. She is currently lecturing with the department of Mathematics at Universitas Negeri Malang, Malang, Indonesia. She is a member of the Engineers and the Institute of Electrical and Electronics Engineers (IEEE) Indonesia Section. Her research areas of interest include data science, natural language processing, and artificial intelligent. She can be contacted at email: denis.eka.cahyani.fmipa@um.ac.id.

Anjar Dwi Hariadi is currently student in Department of Mathematics at Universitas Negeri Malang, Malang, Indonesia since 2019. He is community leader of Google Developer Student Clubs Universitas Negeri Malang for 2022—2023 cohort. His research areas of interest include machine learning, deep learning, and web and mobile application development. He can be contacted at email: anjar.dwi.1903126@students.um.ac.id.

Faisal Farris Setyawan is currently student in department of Mathematics at Universitas Negeri Malang, Malang, Indonesia since 2019. He is core team member of Google Developer Student Clubs Universitas Negeri Malang for 2022—2023 cohort. His research areas of interest include image processing, image classification, data science, object detection, deep learning and machine learning. He can be contacted at email: faisal.farris.1903126@students.um.ac.id.

Langlang Gumilar received the Bachelor of Applied Science (S.ST.) degree in Electromechanic from STTN-BATAN, Indonesia, in 2013 and the Master of Engineering (M.T.) degree in Electrical Engeering from Universitas Indonesia, Indonesia in 2015. Currently, he is a Lecturer at State University of Malang, Department of Electrical Engineering, Indonesia. His interest research is electrical power system, power quality, renewable energy, and energy management. He can be contacted at email: langlang.gumilar.ft@um.ac.id.

Samsul Setumin received the B.Eng. degree (Hons.) in electronic engineering from the University of Surrey, in 2006, and the M.Eng. degree in electrical-electronic and telecommunication from the Universiti Teknologi Malaysia, in 2009. He obtained his Ph.D. degree from Universiti Sains Malaysia in 2019 in the imaging field. Since 2010, he has been a Lecturer with the Universiti Teknologi MARA, Malaysia. He was a Test Engineer with Agilent Technologies (M) Sdn. Bhd., and Intel Microelectronics (M) Sdn. Bhd., for a period of one year. His research interests include computer vision, image processing, pattern recognition, and embedded system design. He can be contacted at email: samsuls@uitm.edu.my.